PHYSICAL REVIEW E **91**, 010201(R) (2015)

Steadily oscillating axial bands of binary granules in a nearly filled coaxial cylinder

Shio Inagaki,[1,*] Hiroyuki Ebata,[1] and Kenichi Yoshikawa[2]
[1]*Department of Physics, Chiba University, Chiba 263-8522, Japan*
[2]*Faculty of Life and Medical Sciences, Doshisha University, Kyoto 610-0394, Japan*
(Received 19 May 2014; published 7 January 2015)

Granular materials often segregate under mechanical agitation such as flowing, shaking, or rotating, in contrast to an expectation of mixing. It is well known that bidisperse mixtures of granular materials in a partially filled rotating cylinder exhibit monotonic coarsening dynamics of segregation. Here we report the steady oscillation of segregated axial bands under the stationary rotation of a nearly filled coaxial cylinder for $O(10^3)$ revolutions. The axial bands demonstrate steady back-and-forth motion along the axis of rotation. Experimental findings indicated that these axial band dynamics are driven by global convection throughout the system. The essential features of the spatiotemporal dynamics are reproduced with a simple phenomenological equation that incorporates the effect of global convection.

DOI: 10.1103/PhysRevE.91.010201 PACS number(s): 45.70.Mg, 64.70.ps

Introduction. Mixtures of granular materials tend to segregate when they are subjected to mechanical agitation such as flowing, shaking, or rotating. Unlike in mixtures of liquids or gases, dissipative interaction among macroscopic particles gives rise to unconventional macroscopic behavior [1,2]. In many industrial processes, such as the processing of food, pharmaceuticals, and chemicals, this spontaneous demixing phenomenon often needs to be avoided and has been the subject of long-standing study [1]. This counterintuitive tendency has also received the particular attention of physicists over the past two decades [2].

One of the most fascinating examples of segregation is demonstrated by a cylinder that is partially filled with grains of different sizes [3]. When mixtures of grains are steadily rotated in a horizontal cylinder around its axis, two types of segregation are seen: radial and axial. As a result of radial segregation, the smaller particles form a radial core along the axis and the larger particles are expelled to the periphery within just a few revolutions. The particles then separate further into alternating bands that are rich in either small or large particles along the axis. Subsequently, a pattern of well-segregated bands slowly merges and coarsens at a logarithmic rate [4], which represents a kind of relaxation into a pattern of macroscopic segregation. Since axial segregation was first reported by Oyama in 1939 [5], it has been extensively studied experimentally [6–10], theoretically [11–13], and numerically [14,15]. Axial segregation and its spatiotemporal pattern dynamics are counterintuitive because there is no obvious driving force for the axial motion in the system. The origin of the driving force of axial motion needs to be identified to gain a deeper understanding of the mechanism of segregation dynamics.

We focus on the axial motion of grains by minimizing the effect of surface flow by nearly filling the cylinder. Our previous study with a nearly filled single cylinder [16] suggested that very slow but steady global convection was present under stationary rotation. In dense granular systems, the very slow collective motion of grains gives rise to macroscopic transport and circulation of the media [16–18]. We adopt a coaxial cylinder to stabilize this global convection by interposing a granular layer between cylinder walls as solid boundary conditions.

The experiments were performed using two types of grains in an acrylic transparent co-axial cylinder [Fig. 1(a)]. The cylinder has inner R_{in} and outer radii R_{out} of 2 and 4 cm [Fig. 1(b)], respectively, and a length L of 34 cm. The smaller particles, silica sand, were 207 ± 67 μm in diameter and white in color, while the larger particles, garnet sand, were 388 ± 173 μm in diameter and dark red (see E in [19]). The angle of repose was 37° (silica sand) and 33° (garnet sand). An equal-volume mixture of the two types of particles was poured into a vertical coaxial cylinder that had one end open. The end was then closed and the cylinder was placed horizontally on two shafts parallel to its axis. The cylinder was rotated at a constant rotation rate Ω by driving one of the shafts by a brushless dc electric motor (Oriental Motors). Digital images of the entire cylinder were taken every 30 s. To make a space-time diagram, the images were cropped to the length of the cylinder and a height of one pixel approximately at the height of the axis of the cylinder. The cropped images were then stacked on top of each other. The fill level was defined as the fraction of cylinder volume that appeared to be filled with particles.

Segregation dynamics. Figure 2 shows the segregation dynamics under representative steady states at approximately 10 and 25 h, respectively, after the start of the experiments. In Fig. 2(a), at a fill level of 0.932, a series of snapshots indicates the generation of traveling waves, where the axial bands of the larger red particles appear one after another at the middle, travel symmetrically toward both sides, and then disappear near the end walls. A similar dynamic

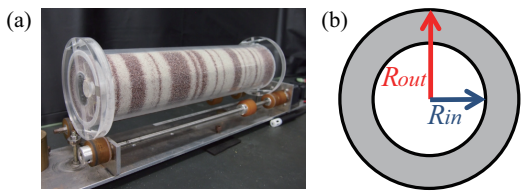

FIG. 1. (Color online) (a) Photo of the experimental setup. (b) Sketch of a lateral image of the coaxial cylinder.

*Corresponding author: inagaki@physics.s.chiba-u.ac.jp

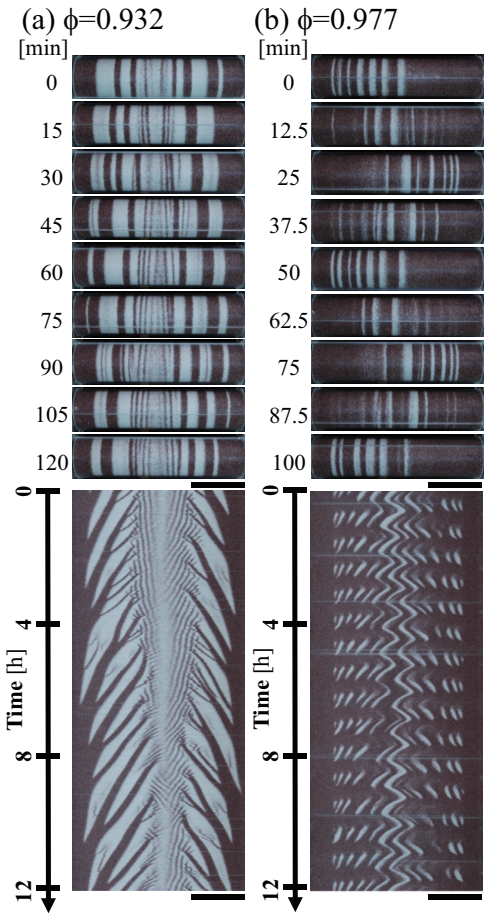

FIG. 2. (Color online) Series of snapshots (top) and spatiotemporal plots (bottom) capturing the exterior segregation patterns at a rotation rate of 27 rpm: (a) traveling waves moving from the center toward both ends, observed at $\phi = 0.932$ and (b) bidirectional steady oscillation of the bands at $\phi = 0.977$. The scale bar indicates 10 cm.

pattern with traveling waves has been observed with a nearly filled single cylinder [16]. In Fig. 2(b), at a fill level of 0.977, a back-and-forth rhythmic band pattern is shown for approximately two oscillations. The narrower bands consist of smaller white particles. Note that all of the bands migrate simultaneously in the same direction, either to the left or right, in a repetitive manner, indicating that the oscillation is not local but rather global throughout the cylinder. The steady oscillating dynamics of the axial bands are shown to be even more evident in the spatiotemporal diagram, the lower panel of Fig. 2(b). It has been confirmed that such back-and-forth oscillation dynamics can be sustained for more than 3 days. Videos of this process are available in A in [19].

Figure 3 shows a phase diagram of the segregation dynamics as a function of the rotation rate and fill level. The surface flow was shown to be steadily and smoothly streaming within the parameter region shown here. Even at high fill levels, surface flow appears because of compaction in the course of the experiment. In every experimental run, the cylinder is rotated for approximately 4 days to confirm the steady dynamics. The dominant parameter is the fill level ϕ and there

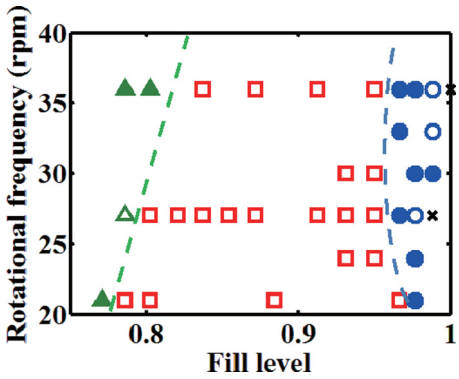

FIG. 3. (Color online) Phase diagram of the spatiotemporal segregation dynamics. The spatiotemporal patterns of segregation can be classified into the following four steady states: monotonic coarsening (open triangle), traveling wave (squares), oscillation (open circles), and ceasing (cross). There are also nonsteady states: intermittent oscillation (closed circles) and monotonic coarsening accompanied by a traveling wave (closed triangles).

is a slight dependence on the rotation rate Ω. At the lowest ϕ, the segregation dynamics show monotonic coarsening, which is similar to that in the case of a partially filled single rotating drum [4]. With an increase in the fill level, traveling waves appeared. When the fill level is set as high as possible, an indistinct solitary band (white) appears in the middle and does not move in any direction (the ceasing pattern). Oscillatory dynamics appears when the fill level is set slightly less than that of the ceasing pattern. The fill level is set slightly less than that of the ceasing pattern and the bands of white particles steadily oscillate over 3 days. The steady oscillatory region is relatively narrow and intermittent oscillation appears in the region around it. In the lowest region of the fill level, there is also a nonsteady state that shows a monotonic coarsening pattern accompanied by a traveling wave near the end wall. The detailed spatiotemporal plots of these states are given in B in [19]. An internal segregation structure is also investigated as shown in C in [19].

Band velocity profiles. Figure 4(a) shows the average band velocity as a function of time and position, which was deduced from the analysis of the space-time plot given in Fig. 2(b). The velocity is shown according to the color map. Time increases downward from the top. The space coordinate is shown on the horizontal axis from -12 to 12 cm. The spatiotemporal plot was in a binary format and the centroid of each band was tracked to obtain the band velocity. Since the oscillation is highly periodic, the data regarding the band velocity were divided by one oscillation period $\tau = 48.7$ min. The band velocity was then averaged over the divided samples in the same phase and position. Data were obtained for 3500 min ($\sim$2.4 days) to ensure that the bands oscillated steadily. We found that there are two vortices in the velocity field that rotate in positive and negative directions, respectively, at the surface of the cylinder. The two velocity vortices inflate and deflate alternately in a periodic manner. These observations suggest that oscillation is accompanied by the two vortices in the velocity field driving each other back and forth, as shown schematically in Fig. 4(b).

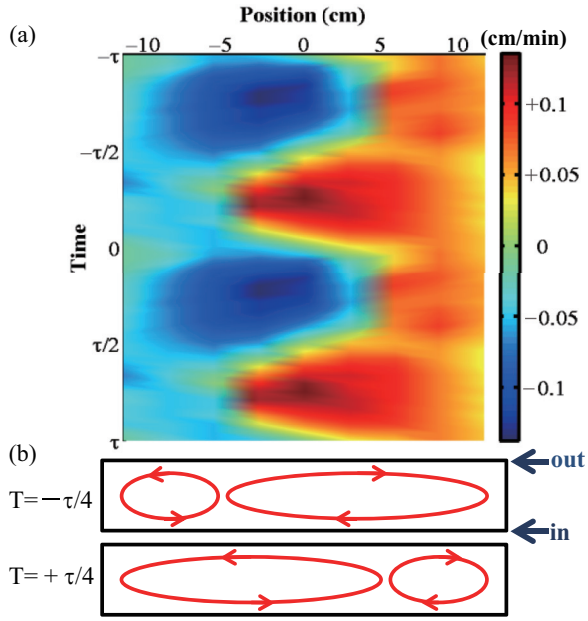

FIG. 4. (Color) (a) Band velocity profile given as a color representation, for a steady oscillation pattern at $\phi = 0.977$ and $\Omega = 27$ rpm. The phase is determined with a period $\tau = 48.7$ min. (b) Schematic drawing of the profile of the velocity field in the coaxial cylinder. The upper part of the cross section (drawn as a rectangle) corresponds to the outer cylinder and the lower part corresponds to the inner cylinder.

Similarly, the velocity profile of the traveling-wave pattern ($\phi = 0.913$) was also analyzed, as shown in Fig. 5(a2). Figure 5(a1) shows the space-time plot of the traveling-wave pattern for a period of 340 min for reference. The band velocity was correlated with its position, but not its width. Thus, the velocity of all the bands was averaged over time at each position. We found that the bands accelerate around the center and slow as they approach the boundary of the convections. The velocity profile was highly symmetric. Based on Fig. 4(a), the velocity profile of the oscillating pattern was plotted as a function of position for different oscillation phases [Fig. 5(c2)]. Figure 5(c1) shows a space-time plot for a period of 340 min. In our experiments, the band velocity is mostly dependent only on its position, irrespective of the difference of the spatial pattern. This suggests that the band dynamics is determined macroscopically through the global convection. Therefore, we adapt an assumption that the band velocity is the same as in the velocity profile of the global convection. Hereafter, we propose a model based on a one-dimensional (1D) Cahn-Hilliard model while adopting the band velocity profiles obtained in these experiments.

Modeling. In our previous work, we proposed a 1D Cahn-Hilliard equation to reproduce the segregation dynamics of a nearly filled single rotating drum [16]. By extending this model, we propose a simple model for the segregation dynamics of a nearly filled coaxial cylinder. First, we focus on the two-phase separation on the surface of the cylinder where the segregated bands appear. We define the fraction of large red particles at X as $c(X) = S_L(X)/[S_L(X) + S_S(X)]$, where $S_L(X)$ and $S_S(X)$ are the local partial volume concentrations

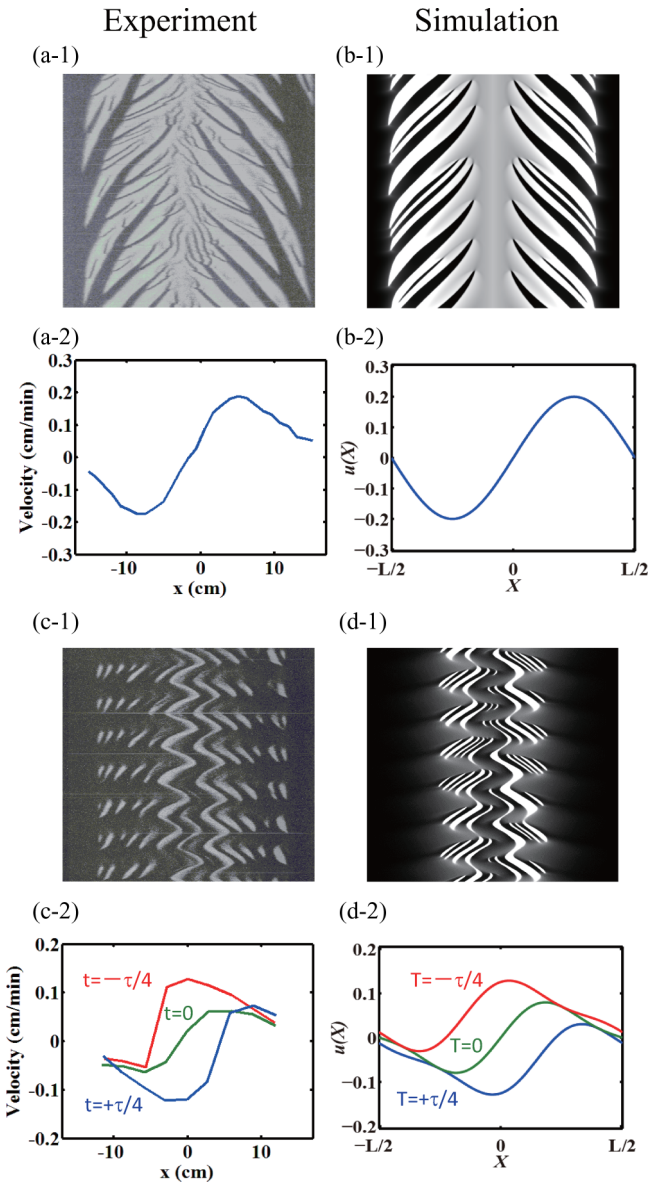

FIG. 5. (Color online) (a1)–(d1) Space-time plots of the segregation dynamics. (a2)–(d2) Band velocity profiles as a function of position. Shown is the traveling wave from (a) experiment ($\phi = 0.913$ and $\Omega = 27$ rpm) and (b) the numerical model and the oscillatory pattern from (c) experiment ($\phi = 0.977$ and $\Omega = 27$ rpm) and (d) the numerical model. The time periods of the spatiotemporal diagrams are (a1) and (c1) 340 min, while those of numerical models are (b1) 140 time units and (d1) 340 time units. The model is numerically solved with the following parameters in the case of a traveling wave (oscillatory pattern, if not identical): time intervals $\Delta T = 5.0 \times 10^{-4}$ (3.125×10^{-4}), cylinder length $L = 8\pi$, space interval $\Delta X = L/400$, $\lambda = 0.225$ (0.18), $\epsilon = 0.0225$, $\alpha = 0.15L/2\pi$ ($0.089L/2\pi$), $u_0 = 0.2$ (0.07), $\beta_0 = 3$, $\beta_1 = 0$ (0.75), $c_1 = -0.15$, $c_2 = 0.3$, and $c_3 = -0.7$.

of the large and small particles, respectively, at X, where X is the spatial coordinate parallel to the axis of the cylinder. The origin represents the middle of the cylinder. We define an order parameter η as $\eta(X) = [c(X) - c_{min}]/(c_{max} - c_{min})$, where c_{max} and c_{min} are the maximum and minimum concentrations

of the phase, respectively. We assume that the velocity profiles of the global convection at the surface obey those obtained from the experiments [Figs. 5(a2) and 5(c2)]. To grasp the essence of dynamic segregation, we consider a simple 1D model of a Cahn-Hilliard-type equation by incorporating the advective term as

$$\partial_T \eta + \partial_X[u(X)\eta] + \alpha \partial_X u(X) = -\lambda \nabla^2[f(\eta) + \epsilon^2 \nabla^2 \eta], \quad (1)$$

where $u(X)$ is the position-dependent velocity, λ is the diffusion constant, ϵ corresponds to the width of the bands associated with the diffusion constant, α is a system-dependent constant, and T is time. The detailed derivation of the model is described in D in [19]. Based on an ordinary Cahn-Hilliard equation, the additional second term on the left-hand side represents advection and the third term represents the inflow and outflow of η if it is positive and negative, respectively. The free energy is defined to also be position dependent, as

$$f(\eta) = -\eta[\eta^2 - (\beta + 1)\eta + \gamma], \quad (2)$$

$$\beta = \beta_0 \left| \frac{X - X_0}{L} \right| + \beta_1, \quad (3)$$

where $\gamma = \beta$ for $\beta \leqslant 1$ and $\gamma = 2\beta - 1$ otherwise, L is the cylinder length, and β_0 and β_1 are constant parameters. Intuitively, this means that a phase of larger particles becomes more stable linearly from $X = X_0$ to the ends of the cylinder. In the case of the traveling wave, X_0 is constant as $X_0 = 0$, whereas in the case of the oscillatory pattern, X_0 oscillates as $X_0 = Lc_1 \sin(\omega T)$, where ω is the time derivative of the oscillation phase and c_1 is a fitting parameter. This is based on the experimental observations that larger particles tend to gather and stay at both ends. The velocity profiles are given [Figs. 5(b2) and 5(d2)] by assuming the system size L and time unit to be the cylinder length and 1 min, respectively. The detailed functional forms are described in D in [19]. These models are numerically solved and the space-time plots are successfully reproduced as shown in Figs. 5(b1) and 5(d1) in the case of a traveling wave and oscillatory pattern, respectively. The diffusion coefficient λ is set at 0.225 for Fig. 5(b2) and 0.18 for Fig. 5(d2). The larger λ means a less dense configuration of the particles. In the case of a lower fill level, the surface flow is expected to be longer and deeper and the particle configuration would be less dense than that in the case of a higher fill level. Thus, the parameters are chosen to be consistent with the observations in the experiments. With regard to a monotonic coarsening pattern, it can be reproduced simply by eliminating the advection term [12,16].

Discussion. By using a coaxial cylinder, when the fill level is varied over a wide range, the emergence of mode bifurcations among a rich variety of spatiotemporal patterns is found (see Fig. S1 in [19]). We observed segregation dynamics similar to those in a single rotating drum, from monotonic coarsening to a traveling wave [16]. The fill level was shown to be crucial to the segregation dynamics. Interestingly, in the present study with a coaxial cylinder, new modes with steady oscillatory behavior are also generated. In previous studies, transient oscillation [20] and standing-wave-like decaying oscillation [10,21] of axial bands were observed. However, the steady oscillating pattern without any apparent source of restoring energy is quite different from those in previous studies.

Our simple model successfully reproduced the experimental observations, suggesting that the segregation dynamics seen here can be decomposed into phase separation and global convection. The axial bands evolve over the surface and are driven by global convection in the axial direction. As a next step, it is of value to seek the origin of global convection and determine whether global convection is driven by an avalanche as supposed in partially filled cases or simply by revolving motion as in rotating fluids. It would also be interesting to examine the possible occurrence of unknown flow instability even for the granules with a single species, inspired by the present study. Currently, there are so many studies on microphase segregation that are frequently interpreted by a Cahn-Hilliard-type model [22]. On the other hand, fluid dynamics have been described based on the Navier-Stokes equation. We hope that our study promotes the extension of physics toward the mostly unexplored but important phenomena, i.e., the cascade of instability on microphase segregation under global convection.

Acknowledgments. This work was supported by Japan Society for the Promotion of Science KAKENHI through Grant Nos. 12J40224, 13J3349, 23240044, and 25103012.

[1] J. C. Williams, Powder Technol. **15**, 245 (1976).
[2] J. M. Ottino and D. V. Khakhar, Ann. Rev. Fluid Mech. **32**, 55 (2000).
[3] G. Seiden and P. J. Thomas, Rev. Mod. Phys. **83**, 1323 (2011).
[4] B. Levitan, Phys. Rev. E **58**, 2061 (1998).
[5] Y. Oyama, Bull. Inst. Phys. Chem. Res. Jpn. Rep. **5**, 600 (1939).
[6] M. Nakagawa, S. A. Altobelli, A. Caprihan, E. Fukushima, and E. K. Jeong, Exp. Fluids **16**, 54 (1993).
[7] V. Frette and J. Stavans, Phys. Rev. E **56**, 6981 (1997).
[8] O. Zik, D. Levine, S. G. Lipson, S. Shtrikman, and J. Stavans, Phys. Rev. Lett. **73**, 644 (1994).
[9] K. M. Hill, A. Caprihan, and J. Kakalios, Phys. Rev. Lett. **78**, 50 (1997).
[10] K. Choo, T. C. A. Molteno, and S. W. Morris, Phys. Rev. Lett. **79**, 2975 (1997).
[11] I. S. Aranson and L. S. Tsimring, Phys. Rev. Lett. **82**, 4643 (1999).
[12] S. Puri and H. Hayakawa, Physica A **270**, 115 (1999).
[13] R. Kobayashi, T. Yanagita, and K. Ueda, J. Soc. Powder Technol. Jpn. **37**, 680 (2000).
[14] D. C. Rapaport, Phys. Rev. E **65**, 061306 (2002).
[15] P. Richard and N. Taberlet, Soft Matter **4**, 1345 (2008).
[16] S. Inagaki and K. Yoshikawa, Phys. Rev. Lett. **105**, 118001 (2010).
[17] H. P. Kuo, P. Y. Shih, and R. C. Hsu, AIChE J. **52**, 2422 (2006).

[18] F. Rietz and R. Stannarius, Phys. Rev. Lett. **100**, 078002 (2008); **108**, 118001 (2012); Phys. Rev. E **85**, 040302 (2012).

[19] See Supplemental Material at http://link.aps.org/supplemental/10.1103/PhysRevE.91.010201 for (A) videos of traveling wave pattern and oscillating dynamics, and (B) space-time plots with various fill levels. It also contains (C) internal segregation structures with various fill levels, (D) derivation of the 1D model, and (E) detailed information of grains used in the experiments.

[20] M. Newey, J. Ozik, S. M. van der Meer, E. Ott, and W. Losert, Europhys. Lett. **66**, 205 (2004).

[21] Z. S. Khan, W. A. Tokaruk, and S. W. Morris, Europhys. Lett. **66**, 212 (2004).

[22] T. Ohta and K. Kawasaki, Macromolecules **19**, 2621 (1986).